

## AIR-WATER FLOW STRUCTURES AT AN ABRUPT DROP WITH SUPERCRITICAL FLOW

H. CHANSON and L. TOOMBES

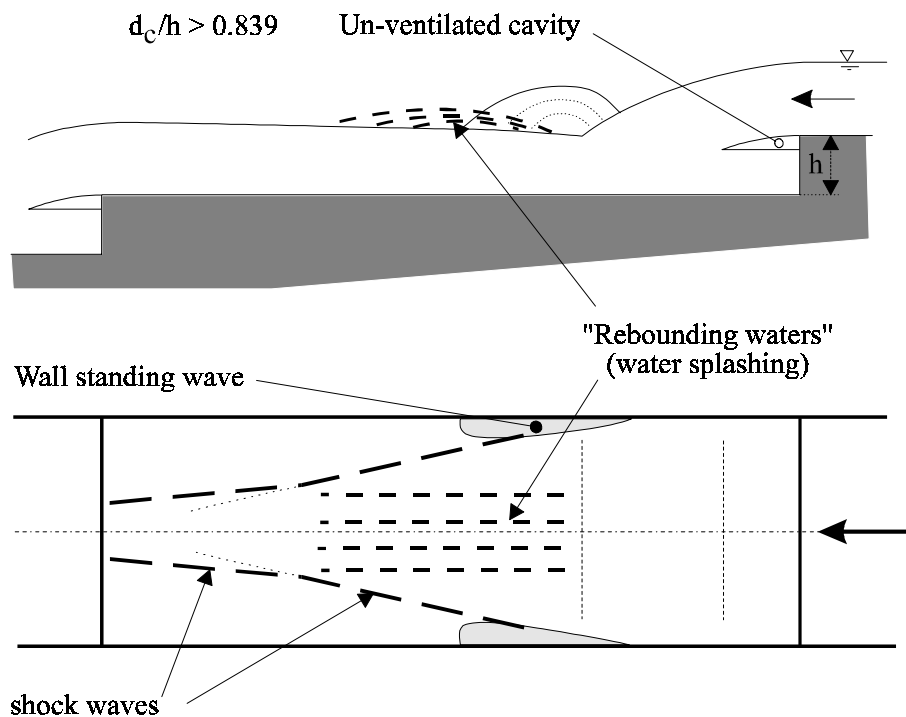
*Department of Civil Engineering, The University of Queensland, Brisbane QLD 4072, Australia*

### 1. Introduction

In storm waterways, at reservoir outlets and in water treatment plants, it is common to design drops, stepped waterways and cascades because of their energy dissipation and flow aeration characteristics. At an abrupt drop, the supercritical flow is characterised by a free-falling nappe impacting on the downstream invert (fig. 1). Substantial flow aeration is observed both in the nappe and downstream of the nappe impact. There is however little information available on the air-water flow characteristics.

It is the purpose of this study to present new information on supercritical flow at an abrupt drop and on the free-surface aeration taking place. The study is based on new experimental data obtained in a large flume at the University of Queensland. The results are later compared with prototype observations at the Gold Creek dam cascade

Fig. 1 - Supercritical flow at an abrupt drop : basic flow patterns



### 2. Experimental facility

The authors conducted new experiments in a 0.5-m wide channel for discharges ranging from 0.038 to 0.163  $\text{m}^2/\text{s}$ . The flume is made of planed wooden boards. The abrupt drop ( $h = 0.131$  m) is located 2.4-m downstream of a wall jet nozzle issuing a 30-mm thick jet. The channel invert, upstream and downstream of the vertical drop, is flat and horizontal.

Water is supplied by a pump with a variable-speed electronic controller enabling a fine discharge adjustment in a closed-circuit system. The water discharge is measured with a Dall™ tube flowmeter and the accuracy on the discharge measurement is about 2%. Clear-water flow depths are measured with a pointer gauge.

Air concentration measurements were performed using a single-tip conductivity probe developed at the University of Queensland (CHANSON 1995). The probe consists of an internal concentric electrode ( $\varnothing = 0.35$

mm) made of platinum and an external stainless steel electrode of 1.42 mm diameter. The probe is excited by an air bubble detector (AS25240) designed with a response time less than 10  $\mu$ s.

The translation of the probe in the direction normal to the channel bottom is controlled by a fine adjustment travelling mechanism connected to a Mitutoyo™ digimatic scale unit (Ref. No. 572-503). The error on the vertical position of the probe is less than 0.025 mm. The system (probe and travelling mechanism) is mounted on a trolley system. The accuracy on the longitudinal position of the probe is less than 1 cm and the accuracy on the lateral position of the probe is less than 1 mm.

Nappe cavity subpressures are recorded with a projection manometer (TEM Engineering™ Ref.: M939). In addition high-speed photographs were taken to analyse the flow patterns. Further details of the instrumentation and the full set of experimental data are reported in CHANSON and TOOMBES (1997a,b).

### Flow conditions

The experiments were performed with inflow velocities ranging from 1.27 to 5.4 m/s. The flow depth downstream of the nozzle was 0.03 m for all the experiments. The flow was supercritical upstream and downstream of the abrupt drop for all the investigated flow conditions. Further the air cavity beneath the nappe was not ventilated (artificially).

Fig. 2 - Photograph of the stepped cascade in operation ( $q_w = 0.132 \text{ m}^2/\text{s}$ )  
Flow from the top to the bottom

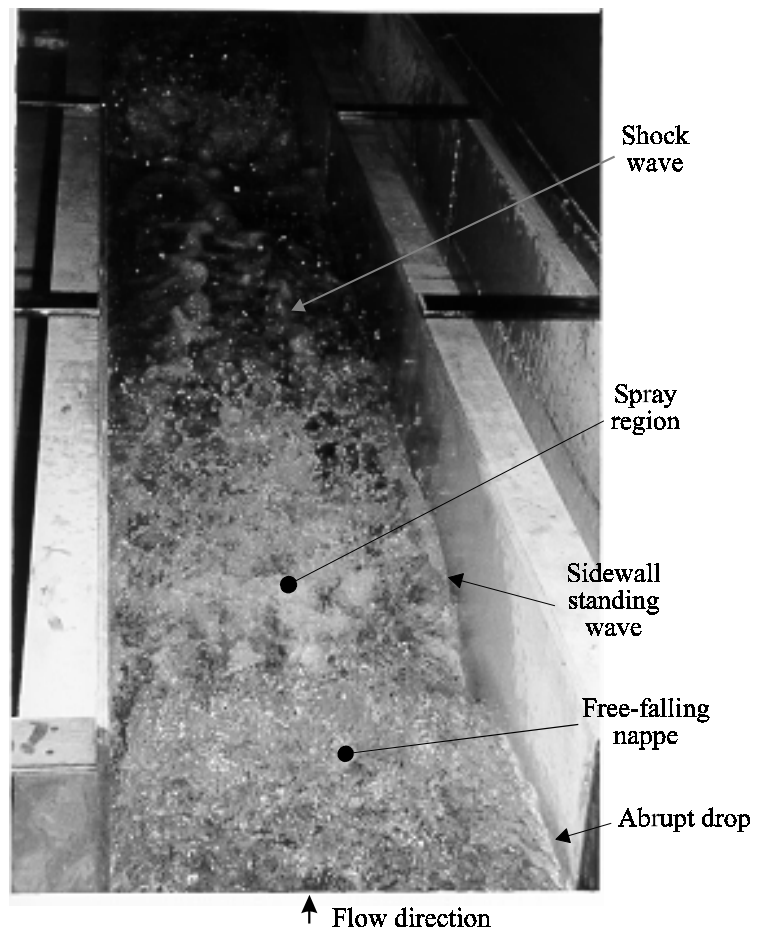
## 3. Air-water flow

### 3.1 Flow patterns

At the abrupt drop, the flow becomes a free-falling jet and the air cavity beneath the nappe is clearly seen although the air cavity is not ventilated. For one particular discharge (i.e.  $q_w \approx 0.163 \text{ m}^2/\text{s}$ ), loud noise was generated by the air cavity. The noise could be reduced by introducing a rod in the nappe, acting as a splitter device.

For all investigated flow conditions, the jet impact induces significant water splashing and jet deflection, followed by the propagation of *oblique shock waves* (i.e. cross-waves) intersecting further downstream on the channel centreline (fig. 1 and 2). The inflow and the free-falling nappe are basically two-dimensional, even so the falling nappe appears to exhibit some contraction away from the wall. Downstream of the nappe impact, the flow becomes three-dimensional. At nappe impact, the flow is characterised by a change of direction in the vertical streamwise plane and by some flow deceleration caused by energy dissipation at the impact. The change of streamline direction induces the propagation of shock waves and some *spray*. The spray is observed across most of the channel width. Water droplets, ejected with the spray, overtop often the channel sidewall (0.4-m high). Visual observations suggest that the rebounding waters (i.e. the spray) re-attach the main stream with impact velocities larger than the mean flow. If this hypothesis is verified, the flow immediately downstream of the impact would be slower than the spray.

*Sidewall standing waves* are observed also at the impact of the nappe along the sidewalls (fig. 1 and 2). The wave height at the wall could be as large as the drop height. Note that the location of maximum height of the wall standing waves does not coincide exactly with the start of the cross-waves.



### 3.2 Effect of air entrainment on shock wave intersection

Different types of *shock wave intersection* are observed in the channel for different flow rates. At low flow rates (i.e.  $q_w < 0.08 \text{ m}^2/\text{s}$ ), the traditional shock wave intersection is observed for which the crosswaves intersect without significant interference. This is typical for supercritical flows in absence of free-surface aeration.

During the present study, flow aeration is significant and the free-surface behind the shock waves is characterised by turbulent wavelets and free-surface aeration. Downstream of the shock wave intersection, the free-surface aeration tends to mask the cross-waves albeit evidence of shock waves can still be seen.

Another type of shock wave intersection is observed only at large flow rates (i.e.  $q_w \geq 0.13 \text{ m}^2/\text{s}$ ). In such a situation, the cross-waves are highly turbulent and aerated. When the shock waves intersect, they merge into a straight standing wave flowing parallel to the walls (fig. 3). This longitudinal standing wave extends over the downstream overfall, interfering with the subsequent step.

Fig. 3 - Photograph of merging shock waves ( $q_w = 0.120 \text{ m}^2/\text{s}$ ) - Flow from the top to the bottom

## 4 Free-surface aeration

### 4.1 Experimental results

Figure 4 shows air concentration data recorded on the centreline and next to the sidewall (1.7-mm from the wall). The nappe trajectory, nappe cavity, spray and sidewall standing waves are shown.

On the channel centreline, figure 4 indicates significant interfacial aeration along both the upper and lower nappes. At the end of the free-jet and immediately upstream of the impact point, the nappe is highly aerated including along the jet core where  $C > 0.1$ . Downstream of the impact point, significant free-surface aeration takes place in the spray region (fig. 4). The authors feel however that the slip velocity might not be unity in the spray and hence the spray data should be read as the ratio of average time spent by the probe tip in air to the total scanning time (rather than void fraction).

Next to the sidewall, the contraction of the free-falling nappe induces a thin gap between the wall and the water jet, allowing natural ventilation of the nappe. This is seen on the air concentration data at 1.7-mm from the wall. Further the sidewall standing waves are clearly shown in figure 4. Note in particular the extent of the wall waves and their high air contents. Visually the sidewall standing waves have a "frothy" foamy appearance.

### 4.2 Discussion

Dominant features of the air-water flow are the large air-cavity beneath the nappe, the free-surface aeration of the jet interfaces, substantial flow aeration in the spray region and the de-entrainment at the spray re-attachment.

Figure 5 presents the longitudinal variation of the average air content (defined in terms of 90% air content) downstream of the nappe impact. In figure 5,  $C_{\text{mean}}$  is plotted as a function of the dimensionless distance  $x/l$ ,  $x$  being measured from the vertical step face and positive in the downstream direction, and  $l$  being the distance to the downstream overfall ( $l = 2.4 \text{ m}$ ). The results show that the mean air content is maximum downstream of the nappe impact (in the spray region) and minimum at the downstream end of the step (fig. 5).

A comparative analysis was developed between experimental data obtained with the abrupt drop flume (4.8-m long) and with a smooth chute (invert slope : 4 deg.) (CHANSON and TOOMBES 1997b). The results indicate that the abrupt drop flow is aerated very rapidly at the drop and that, at the downstream end, the mean air content is about 0.20 for  $q_w = 0.15 \text{ m}^2/\text{s}$ . In comparison the mean air content at the downstream end of the smooth chute was about 0.12 (at  $x = 4.8 \text{ m}$ ). The stepped chute flow is significantly more aerated than the smooth chute flow for the same flow rate and this result is visually observed. Another difference is the three-dimensional flow pattern of the stepped channel (the smooth chute flow is two-dimensional).

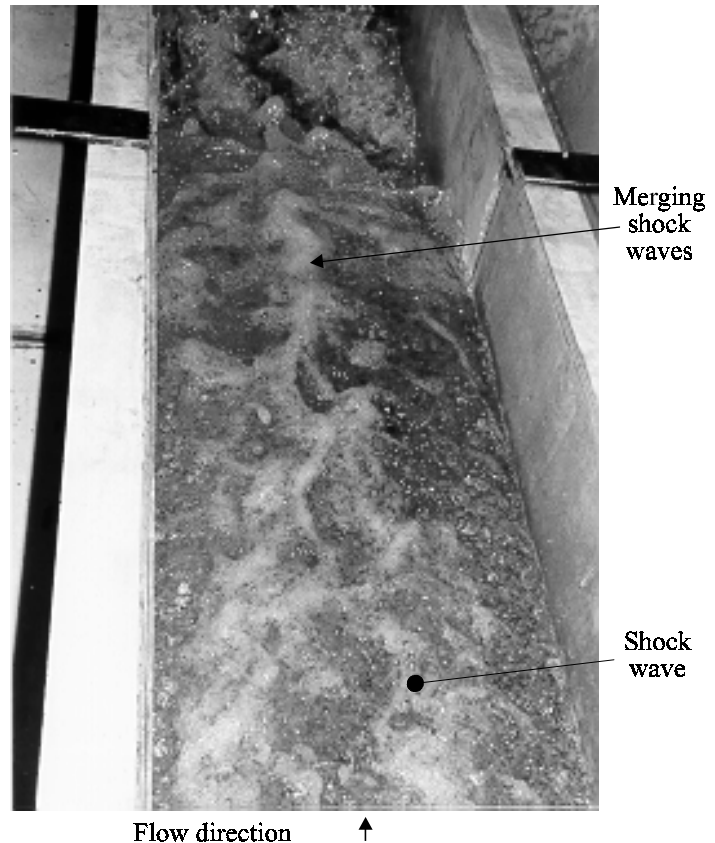


Fig. 4 - Air entrainment in a supercritical flow at an abrupt drop ( $q_w = 0.15 \text{ m}^2/\text{s}$ ,  $V_o = 5 \text{ m/s}$ ,  $h = 0.131 \text{ m}$ )

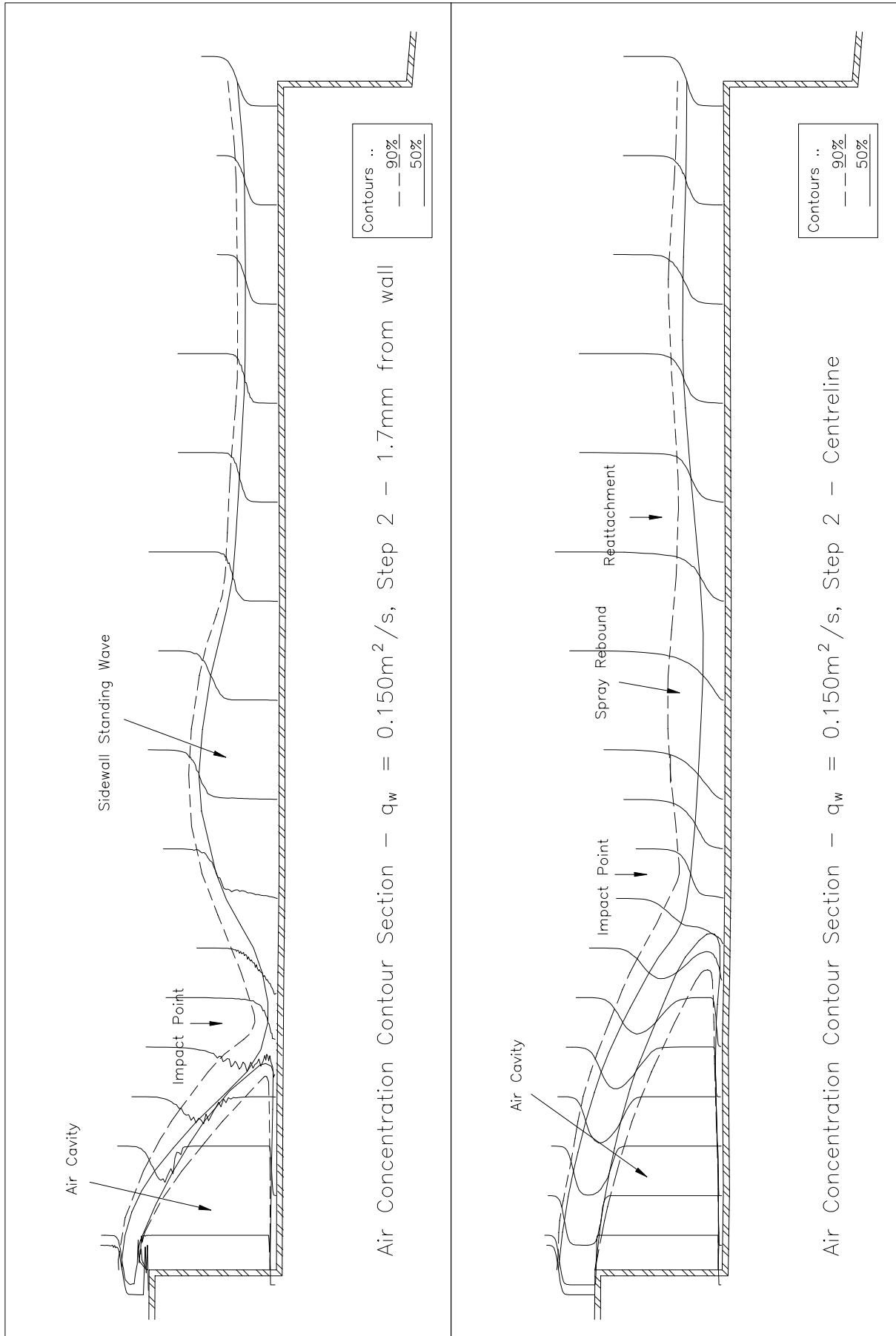
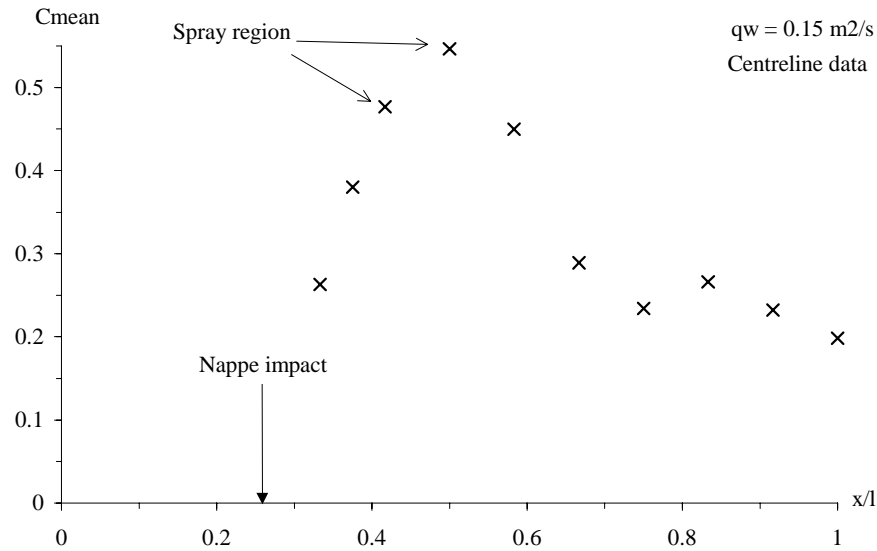


Fig. 5 - Mean air concentration along a step on the channel centreline



## 5. Discussion

### 5.1 Application to chute design

Practically the substantial flow aeration of the free-jet, sidewall standing waves and spray region may affect the design of chute sidewall. The flow bulking resulting from air entrainment leads to the design of higher sidewalls. Further the large amount of entrained air has a significant impact on the downstream water quality. The air-water gas transfer contribution of the entrained air bubbles is predominant. Stepped cascades and drops are well-known for their potential to re-oxygenate depleted waters.

### 5.2 Prototype observations

The senior author was involved in the study of a prototype stepped cascade (Gold Creek dam spillway, Brisbane, Australia). On the 2 May 1996, a  $0.49\text{-m}^2/\text{s}$  flow discharged over the 1.5-m high steps and colour photographs were taken with a 35-mm camera (CHANSON and WHITMORE 1996).

The analysis of the photographs indicate that the flow at the first drop is basically two-dimensional and it becomes three-dimensional on the downstream invert. Further the flow is highly aerated (i.e. 'white waters') and, at the end of the chute, the air-water flow has a *foam* appearance. Free-surface discontinuities are also observed : they are characteristic of shock waves intersecting next to the step edges. The presence of shock waves and shock wave intersections in prototype reinforce the laboratory findings.

## 6. Conclusion

At an abrupt drop, free-surface aeration takes place predominantly along the free-jet interfaces. Three-dimensional flow patterns are also observed : i.e., shock waves and sidewall standing waves. The characteristics of shock waves and standing waves are related to the downstream Froude number and there is some similarity with abrupt expansion supercritical flows.

Air concentration measurements highlight the substantial aeration at both the lower and upper nappes of the free-falling jet. The data indicate also a large amount of entrained air in the spray region and in the sidewall standing waves. In the spray region the authors feel that the slip velocity might not be unity and the air-water mixture is not homogeneous.

The abrupt flow is highly aerated and the flow aeration affects the shock wave patterns. The laboratory investigation shows the presence of three-dimensional air-water flow structures. Similar results were observed in prototype (i.e. Gold Creek dam spillway). The physics of the flow is not yet fully-understood and additional investigations must be undertaken to characterise the air-water flow characteristics of the entire three-dimensional flow field. More information is still required to predict more accurately the rate of energy dissipation, the rate of air-water gas transfer and the re-oxygenation characteristics of stepped cascades.

## 7. Acknowledgments

The authors thank Dr John MACINTOSH (Water Solutions, Brisbane) for his helpful comments and for reviewing the report.

## 8. References

- CHANSON, H. (1995). "Air Bubble Entrainment in Free-surface Turbulent Flows. Experimental Investigations." *Report CH46/95*, Dept. of Civil Engineering, University of Queensland, Australia, June, 368 pages.
- CHANSON, H., and TOOMBES, L. (1997a). "Energy Dissipation in Stepped Waterway." *Proc. 27th IAHR Congress*, San Francisco, USA, Vol. D, F.M. HOLLY Jr. and A. ALSAFFAR Ed., pp. 595-600.
- CHANSON, H., and TOOMBES, L. (1997b). "Flow Aeration at Stepped cascades." *Research Report No. CE155*, Dept. of Civil Engineering, University of Queensland, Australia, June, 110 pages.
- CHANSON, H., and WHITMORE, R.L. (1996). "Investigation of the Gold Creek Dam Spillway, Australia." *Research Report No. CE153*, Dept. of Civil Engineering, University of Queensland, Australia, 60 pages.